Studies of excited state charge-transfer interactions with picosecond laser pulses

T. J. Chuang and K. B. Eisenthal

IBM Research Laboratory, Monterey and Cottle Roads, San Jose, California 95193
(Received 17 October 1974)

The methods of picosecond laser photolysis have been employed to study the inter- and intramolecular charge-transfer interaction between excited anthracene and *N*,*N*-diethylaniline in polar as well as nonpolar solvents. The formulation of reaction kinetics coupled with molecular reorientational motion is developed. The experimental results, at low diethylaniline concentrations, are analyzed in terms of diffusion model and Noyes molecular pair model. The transient behavior due to instantaneous flux in early time regions is clearly evident. The values of critical intermolecular distance and primary rate constant for electron transfer are determined and are consistent for all solutions studies. In the high diethylaniline concentration region, analysis of orientational relaxation times and the rate of charge-transfer reactions clearly reveals the dynamic nature of the interacting processes.

I. INTRODUCTION

The understanding of the mechanism of inter- and intramolecular quenching of fluorescence is of fundamental importance in the study of the primary photophysical and photochemical processes of the excited aromatic hydrocarbons. One of the major quenching mechanisms is due to the excited state charge-transfer interactions. The charge transfer process which we are considering occurs between excited and ground state molecules and not between ground state molecules. The transfer of an electron from the donor molecule D to the excited acceptor molecule A* quenches the normal A* fluorescence, gives rise to a new emission in low dielectric solvents, can produce ion radicals, provide new pathways for energy degradation, and can change the chemistry of the system. The physical and chemical nature of these diverse processes have been extensively studied since the discovery of excited state charge transfer complexes by Leonhardt and Weller,[1] but heretofore not in the subnanosecond time region which is of key importance to an understanding of these events. In addition to our interest in the charge transfer process and the subsequent energy dissipation, the electron transfer reaction between A* and D provides an excellent vehicle for testing the theories of diffusion controlled chemical reactions.

Depending on solvent polarity, there can be two different mechanisms involved in the electron-transfer reactions. In solvents of high polarity, a more or less strongly solvated radical ion pair is formed upon photoexcitation of the electron acceptor (A) or the donor (D), i.e.,

$$^1A + {}^1D \xrightarrow{h\nu} {}^1A^* + {}^1D \xrightarrow{k_i} {}^2A_s^- \text{---} {}^2D_s^+ \quad . \tag{1}$$

In this process, the fluorescence of the excited species is strongly quenched and there is very little emission from the solvated ion pair whose ions are in their doublet ground states. The ion pair can subsequently be dissociated, particularly in very polar solvents, into two separated ions and relaxed into triplet and/or ground states. In solvents of low polarity, however, the quenching of fluorescence of the excited aromatic hydrocarbon is coupled with the appearance of a new structureless broad emission band about 5000 cm^{-1} red shift from the original fluorescence. This emission band is attributed to a charge-transfer (CT) complex formed in the excited state, i.e.,

$$^1A^* + {}^1D \xrightarrow{k_{CT}} {}^1(A^-D^+) \quad . \tag{2}$$

Unlike the solvated ion pair which does not have a strong geometrical preference, the charge-transfer complex most probably has a sandwich structure.[2] The complex decays by intersystem crossing into the triplet and via radiative and other nonradiative processes to the ground states.

Although the physicochemical processes involved in the charge-transfer interaction systems have been qualitatively established, important problems regarding the dynamic nature of molecular motion[3] and geometrical requirement[4,5] for interaction, and the mechanism of the generation of locally excited triplet states[6,7] remain to be elucidated. In the earlier report,[3] we demonstrated the capability of picosecond laser techniques in answering some of these crucial questions. We present here the experimental results in this continuing effort. In particular, we want to see whether there are differences in reaction dynamics between the ion pair [Eq. (1)] and charge-transfer complex [Eq. (2)] formations, and their subsequent decays. The decays of these excited species are related to the triplet state formation, a controversial and unresolved subject.[6,7] Meanwhile, we have also carried out a picosecond study of the charge-transfer interactions in antrhacene-$(CH_2)_3$-N, N-dimethylaniline systems.[8] We established the importance of reorientational motion of the molecules in the charge-transfer interactions. All these experimental results are related. They converge into a clear picture whose features will be discussed in this paper.

II. EXPERIMENTAL

The picosecond ruby laser system is shown in Fig. 1. A ruby rod ($\frac{3}{8}$ in × 5) was pumped by a helical flash lamp in a water-cooled laser head (Korad K1 system). The laser oscillation was mode-locked by a circulating meth-

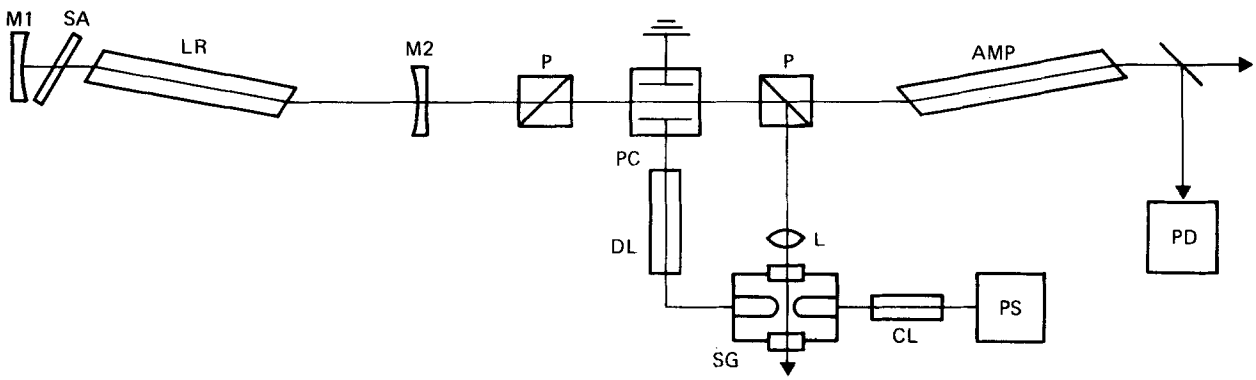

FIG. 1. Schematic of laser oscillator, single pulse selector and amplifier. M1, M2-laser mirrors; SA-saturable absorber; LR-laser rod; P-polarizer; PC-Pockels cell; DL-delay line; L-lens; CL-charging line; SG-spark gap; PS-power supply; AMP-amplifier rod; PD-photodiode.

anol solution of 1, 1′-diethyl-2, 2′-dicarboncyanine iodide. A train of about 30 pulses, separated by the round trip time of the cavity, i.e., 8 nsec, was produced at the output of the oscillator. The energy of the light pulse at 6943 Å was of the order of 1 mJ. A single light pulse was extracted from this train of pulses using a pair of crossed polarizers, and a Pockels cell triggered by the laser induced breakdown of a spark gap filled with nitrogen.[9] Selection of almost any desired pulse could be achieved by adjusting the gas pressure and electrical delay line. The extracted pulse was then amplified by two flash lamp pumped ruby rods (same dimensions). Each had an amplification factor of 4~5. The typical pulse train and the single light pulse so obtained are shown in Fig. 2. The laser pulse width (FWHM) was measured by two photon excited fluorescence methods (TPF),[10] using a methanol solution of rhodamine 6G as the two photon absorbing medium. The experimental setup and results are shown in Fig. 3. The pulse width was determined to be 7 psec. However, we also observed pulse width variations extending up to 15 psec. The light pulse was then frequency doubled to 3472 Å using an appropriately cut KDP crystal. The second harmonic pulse excited the electron acceptor, anthracene, to its first excited singlet state ($^1B_{2u}^+$). Upon transfer of an electron from the donor to the acceptor, a new absorption could be detected at 6943 Å region corresponding to the $(A^- - D^+) \rightarrow (A^* - D^+)$ transition.[11] The experimental arrangement was published earlier.[3,8]

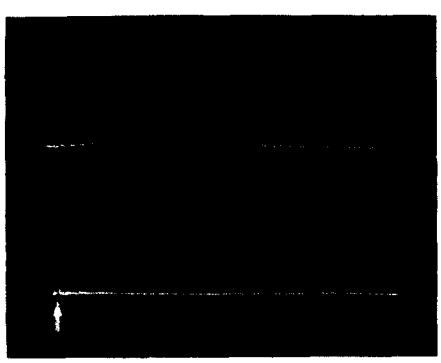

FIG. 2. Laser pulse train (upper trace) and a selected single light pulse as indicated by an arrow (lower trace). The pulses in the pulse train are separated by 8 nsec.

In this way the transfer of an electron leading to the formation of a negatively charged acceptor, either in the ion pair or the CT complex reaction, was monitored by measuring the absorption of the 6943 Å probe pulse at times equal and subsequent to the 3472 Å excitation pulse. The excitation light pulse was linearly polarized. To obtain the dynamics of reorientational motion of molecules involved, polarizers were used before and after the sample so that both the transmissions of the probe light polarized parallel ($I_\parallel/I_0$) and polarized perpendicular ($I_\perp/I_0$) to the electric vector of the excitation pulse were measured. These intensities were monitored by a fast response ITT photodiode and a Tektronix 519 oscilloscope. The result at each point in time was an average of five laser shots. The photodiode and oscilloscope were also used for measuring the fluorescence lift times of anthracene and charge-transfer complex excited by a single 3472 Å pulse.

Materials employed were anthracene (Aldrich, zone refined), N, N-diethylaniline (Eastman, redistilled under nitrogen), n-hexane, and acetonitrile (Matheson, Coleman and Bell, spectroquality) and anthracene-$(CH_2)_3$-N, N-dimethylaniline which was prepared from 9-anthraldehyde and 4-dimethylaminoacetophenone.[8]

The concentration of anthracene (A) was fixed at 2.5×10^{-3} M and either n-hexane or acetonitrile was added to vary the diethylaniline (DEA) concentration. All solutions were saturated with nitrogen to avoid oxygen quenching processes. Unless indicated, all experiments were carried out at room temperature.

III. THEORETICAL

A. Reaction kinetics

The general scheme of charge-transfer interaction following photoexcitation of the acceptor is given by

$$A + D \xrightarrow{h\nu} \underset{k_A}{A^*} + D \xrightarrow{f(t)} \underset{k_f}{A^- - D^+}, \qquad (3)$$

where $f(t)$ is the rate function of electron-transfer causing the formation of either an ion pair or a CT complex, k_f is the decay rate constant of A^- or $(A^- - D^+)^*$, k_A is the decay rate constant of A* in the absence of D, and n_A and n_c are the concentrations of A* and A^-, re-

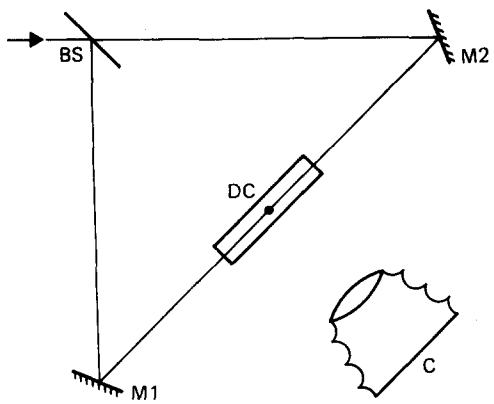

FIG. 3. Experimental arrangement for TPF measurement. BS-beam splitter; M1, M2-mirrors; DC-fluorescence dye cell; C-camera. The TPF photo is also shown. The length of entire trace is 5 cm and the width of the TPF spot is about 1.5 mm.

spectively. $n_c(t)$ is the total concentration of A^-, whether as a separated ion or in the ion pair or in the CT complex. After an instantaneous exciting light pulse, the rate equations can be given by

$$\dot{n}_A = -[k_A + f(t)]n_A \quad , \tag{4}$$

$$\dot{n}_c = f(t)n_A - k_f n_c \quad , \tag{5}$$

and the solutions are

$$n_A(t) = n_A(0)\exp\left[-k_A t - \int_0^t f(t')dt'\right] \quad , \tag{6}$$

$$n_c(t) = n_A(0)e^{-k_f t}\left\{\int_0^t dt' f(t')\exp\left[-(k_A - k_f)t' - \int_0^{t'} f(t'')dt''\right]\right\} , \tag{7}$$

where $n_A(0)$ is the concentration of A* at $t = 0$, i.e., right after the exciting pulse. In all cases studied, k_f is negligibly small in comparison with $f(t)$ and in the time range of measurements $k_f t$ is essentially zero. Furthermore, except in hexane solution of A–$(CH_2)_3$–DMA, k_A is negligible in comparison with $f(t)$. Thus, Eq. (7) can be simplified to

$$n_c(t) = n_A(0)\left[1 - \exp\left(-\int_0^t f(t')dt'\right)\right] . \tag{8}$$

B. Reaction kinetics coupled with rotational diffusion

When a molecular system is excited by light, a nonuniform orientational distribution with respect to the transition dipole moments of the ground and excited state molecules can be created. Therefore, the subsequent measurement of fluorescence intensity or absorbance of the system will be a function of not only the kinetics of a physicochemical process, but also the rotational motion of the molecules. This consideration is particularly important in picosecond spectroscopy where linearly polarized light is used and the rate of molecular reorientation is comparable to the rates of the processes of interest. For the present purpose, the observed transmission of the probe light (6943 Å) are given by

$$I_{\parallel}(t)/I_0 = \exp\left[-\epsilon_c l \int_\Omega N_c(\Omega, t)\alpha_{\parallel}(\Omega)d\Omega\right] \tag{9a}$$

and

$$I_{\perp}(t)/I_0 = \exp\left[-\epsilon_c l \int_\Omega N_c(\Omega, t)\alpha_{\perp}(\Omega)d\Omega\right] \tag{9b}$$

where ϵ_c is the absorption coefficient of A^-, l is the length of the optical path, $N_c(\Omega, t)$ is the concentration of A^- with its transition vector oriented at an angle Ω at time t, and α's are the projections of this vector along the parallel and perpendicular laboratory axes which are defined by the electrical vector and the direction of propagation of the exciting pulse. $N_c(\Omega, t)$ and $n_c(t)$ are related by

$$n_c(t) = \int_\Omega N_c(\Omega, t)d\Omega \quad . \tag{10}$$

We define, in Fig. 4, (X, Y, Z) as laboratory fixed axes, μ_A as the transition dipole $(A \rightarrow A^*)$ fixed in the molecular frame of the acceptor A, μ_c as the transition dipole $(A^- \rightarrow A^{-*})$ fixed in the molecular frame of A^-, and λ as the angle between μ_A and μ_c. Both the excitation and probe pulses travel along Y. However, the exciting pulse is polarized along Z and the probe pulse along Z and X. Thus,

$$\alpha_{\parallel}(\Omega) = |\mu_c \cdot Z|^2 \quad , \tag{11a}$$

$$\alpha_{\perp}(\Omega) = |\mu_c \cdot X|^2 \quad . \tag{11b}$$

We realize that μ_A is excited symmetrically about the Z axis and this symmetry is maintained for all time regardless of the rotational motion of the molecule. Since μ_c is fixed with respect to μ_A, it is symmetrically distributed about Z all the time also. Therefore, $|\mu_c \cdot Y|^2$ equals $|\mu_c \cdot X|^2$ and it follows that

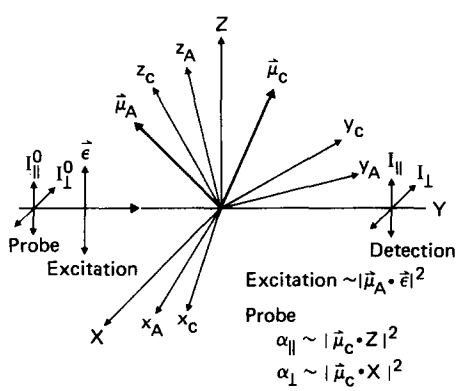

FIG. 4. Experimental geometry: (X, Y, X) are laboratory fixed zxes; (x_A, y_A, z_A) are body fixed axes of A molecule; (x_c, y_c, z_c) are body fixed axes of A^-; μ_A is the transition dipole fixed in A; μ_c is the transition dipole fixed in A^-; both excitation and probe pulses travel along Y, the former polarized along Z, and the latter polarized along Z and X.

$$\alpha_{\parallel}(\Omega) + 2\alpha_{\perp}(\Omega) = 1 \quad . \tag{12}$$

From Eqs. (9) and (10), it follows immediately that the following function

$$(I_{\parallel}/I_0)(I_{\perp}/I_0)^2 = \exp\{-\epsilon_c l n_c(t)\} \tag{13}$$

directly monitors the formation function of A^- in the charge-transfer interaction, or for that matter, any type of rate function of interest. In other words, the sum of the absorbances in one parallel and two perpendicular components is directly proportional to the total concentration of A^- oriented in all directions and therefore is independent of the rotational motion of the molecules. Eq. (13) is applicable to any type of physical or chemical process.

To obtain the dynamics of rotational relaxation, we can employ the general method developed previously for the theory of fluorescence depolarization. [12] We can consider the most general situation in which there are a set of anisotropic rotational diffusion constants for A (D_x^A, D_y^A, D_z^A) and another set for A^- (D_x^c, D_y^c, D_z^c). The two sets of molecular axes are not coincident, and μ_A and μ_c are fixed somewhere in these frames. The resultant functions are very complicated and unless $f(t)$ in Eq. (3) is a constant no closed forms can be obtained. Even then, the expressions for $I_{\parallel}/I_0$ and $I_{\perp}/I_0$ contain more than 20 exponential functions, and are not directly useful. For all practical purposes, we will consider only the case of isotropic rotational diffusion here. The rotational diffusion equation and its solution by Green's function method were shown earlier. [12] Let D be the diffusion constant, $\omega(\Omega, t)$ the probability that the vector of a transition moment is oriented in the angle (Ω) at the time t, $\omega(\Omega_0)$ the similar probability at $t = 0$, and $G(\Omega_0|\Omega, t)$ the Green's function that describes the rotation of the transition vector from Ω_0 at $t = 0$ into Ω at t. We use the subcripts A and c for the acceptor A and A^- molecular systems, respectively, e.g., $\omega_A(\Omega, t)$, $\omega_c(\Omega, t)$, D_A, D_c, and $G_A(\Omega_0|\Omega, t)$ and $G_c(\Omega_0|\Omega, t)$, etc. Once excited, A* reorients according to D_A. At time t', i.e., between $t = 0$ and time of probe t, reaction occurs and the molecule reorients according to D_c. Therefore, $N_c(\Omega, t)$ can be given by

$$N_c(\Omega, t) = \int_0^t \dot{n}_c(t')dt' \int_{\Omega'} \omega_A(\Omega', t')G_c(\Omega', t'|\Omega, t)d\Omega' \quad , \tag{14}$$

where $\dot{n}_c(t')$ is the rate of A^- formation at time t'. Without losing any generality we let the vector μ_A be coincident with one of the molecular axes, say z in Fig. 4, and q_x, q_y, q_z be the projections of μ_c along the molecular axes (x, y, z). The transformation between the laboratory fixed and molecular axes may be given by

$$X = Tx \quad , \tag{15}$$

where the transformation matrix is expressed in terms of the Euler angles (θ, ψ, ϕ). [13] Thus.

$$\alpha_{\parallel}(\Omega) = (q_x T_{Zx} + q_y T_{Zy} + q_z T_{Zz})^2 \quad , \tag{16a}$$

$$\alpha_{\perp}(\Omega) = (q_x T_{Yx} + q_y T_{Yy} + q_z T_{Yz})^2 \quad , \tag{16b}$$

with $q_x^2 + q_y^2 + q_z^2 = 1$. We recognize that in powerful laser excitation, the initial distribution function of μ_A, i.e., $\omega_A(\Omega_0)$, may not be a linear function of $\cos^2\theta_0$. Knowledge of the exact fundamental form of $\omega_A(\Omega_0)$ is not necessary for our derivation, as long as we know that μ_A is excited symmetrically about the Z axis and therefore $\omega_A(\Omega_0)$ is a function of $\cos^2\theta_0$ and independent of angle ψ or ϕ. Using Eq. (14), we can rewrite the integral in Eq. (9a) as

$$y_{\parallel} = \int_0^t \dot{n}_c(t')dt' \int_{\Omega} \alpha_{\parallel}(\Omega)d\Omega \int_{\Omega'} G_c(\Omega', t'|\Omega, t)d\Omega'$$
$$\times \int_{\Omega_0} \omega_A(\Omega_0)G_A(\Omega_0|\Omega', t')d\Omega_0 \tag{17}$$

We expand the Green's functions in terms of the stationary state eigenfunctions and eigenvalues for the asymmetric rigid rotor. In turn, these eigenfunctions are expressed in terms of symmetric rotor wavefunctions and then the Wigner rotation matrices. [12] We obtain for Eq. (17),

$$y_{\parallel} = \tfrac{2}{3}\sqrt{\pi} \int_0^t dt' \dot{n}_c(t') \Big\{ \chi_{0,0} + \frac{1}{\sqrt{5}} \chi_{2,0}(3q_z^2 - 1)$$
$$\times \exp[-6D_c t - (6D_A - 6D_c)t'] \Big\} \quad , \tag{18a}$$

and the equivalent expression for $\alpha_{\perp}(\Omega)$ component as,

$$y_{\perp} = \tfrac{2}{3}\sqrt{\pi} \int_0^t dt' \dot{n}_c(t') \Big\{ \chi_{0,0} - \frac{1}{2\sqrt{5}} \chi_{2,0}(3q_z^2 - 1)$$
$$\times \exp[-6D_c t - (6D_A - 6D_c)t'] \Big\} \quad , \tag{18b}$$

where

$$\chi_{l,0} = \int_{\Omega_0} d\Omega_0 \omega_A(\Omega_0) Y_{l,0}(\Omega_0) \quad ,$$

$Y_{l,0}(\Omega_0)$ is the normalized spherical harmonic function, $\chi_{0,0}$ equals $\frac{1}{2}\sqrt{\pi}$ and $\chi_{2,0}$ is a nonzero constant relating to the power of the light pulse and the oscillator strength of the transition dipole. We should point out that Eqs. (18a) and (18b) can also be obtained using spherical coordinates instead of Euler angles. The Green's function can then be expanded in terms of spherical harmonic functions. We can do this because the rotational motion is isotropic and the exact orientation of the molecular axes is irrelevant. Substituting Eqs. (18a) and (18b) into Eqs. (9a) and (9b) it can be shown readily that the quantity $(I_{\parallel}/I_0)(I_{\perp}/I_0)^2$ is independent of molecular rotation, consistent with Eq. (13). To obtain the diffusion constants, we take the ratio of the component transmissions, i.e.,

$$R = I_{\parallel}/I_{\perp} = \exp\Big\{ -\frac{\pi}{\sqrt{5}} \epsilon_c l \chi_{2,0}(3\cos^2\lambda - 1)\exp(-6D_c t)$$
$$\times \int_0^t \dot{n}_c(t')\exp[-(6D_A - 6D_c)t']dt' \Big\} \quad . \tag{19}$$

We have replaced q_z^2 by $\cos^2\lambda$ where λ is the angle between the transition moment of A and A^-. In certain cases, λ can be evaluated from experimental values of R. In the case that D_A equals D_c, Eq. (19) can be reduced to

$$R = \exp\Big[-\frac{\pi}{\sqrt{5}} \epsilon_c l \chi_{2,0}(3\cos^2\lambda - 1)\exp(-6D_c t) n_c(t) \Big] \quad . \tag{20}$$

In any event, $n_c(t)$ and $\dot{n}_c$ can be obtained experimentally

from Eq. (8), and the diffusion constants can be evaluated from Eq. (19) or (20).

C. Rate functions of electron-transfer

The rate functions of charge-transfer interactions, i.e., $f(t)$ in Eq. (3), can be expressed in several forms depending on experimental conditions and the physical models employed in deriving these expressions. By far the most widely used and discussed model of reaction kinetics is that of diffusion process.[14,15] By solving the translational diffusion equation, i.e., Fick's second law, one is able to obtain the rate of reaction for a bimolecular interacting system as[14]

$$\Phi = \frac{4\pi\rho D' C}{1 + 4\pi\rho D'/k}\left[1 + \frac{k}{4\pi\rho D'}\exp(x^2)\operatorname{erfc}(x)\right] , \tag{21}$$

where

$$x = (1 + k/4\pi\rho D')\sqrt{D't}/\rho , \tag{22}$$

In these equations, ρ is the radius of reacting sphere, D' is the sum of translational diffusion constants of the two molecules, C is the concentration of DEA in this case, and k is the elementary rate constant such that

$$\Phi = kC_\rho , \tag{23}$$

where C_ρ is the concentration of DEA at an intermolecular distance equal to ρ. Eq. (21) clearly indicates there are transient terms in the rate function. The origin of the transient terms and the general time dependence of the chemical reaction can be viewed in the following way. At time $t = 0$, the molecules A* and D are randomly distributed but as time proceeds those distributions in which an A* is near a D are preferentially depleted since there is a higher probability for reaction than for those distributions in which A* and D are far apart. This produces a spatially non-uniform distribution of molecules leading to a flux of molecules from the more concentrated regions of the liquid. Since the distribution of molecules is changing with time, the rate "constant" for the reaction is also changing with time. To adequately test theory and its limits, it is necessary to determine the full behavior of the chemical reaction. The full transient behavior could not be adequately examined prior to the development of picosecond methods[1,14,15,16] and are particularly inportant for the cases studied here.

In an attempt to obtain the reaction rate function in the most general fashion, Noyes developed the reacting pair model, in which the behavior of a pair of moving particles and the probabilities of various types of encounters are analyzed.[14] The rate function so obtained is

$$k_t = kC\left(1 - \int_0^t h(t')dt'\right) , \tag{24}$$

where k and C have the same meaning as indicated earlier and $h(t')dt'$ is the probability that a pair of molecules that encounter without reaction at $t = 0$ will react with each other at t'. The function $h(t')$ cannot be measured directly, however, and Noyes then assumed that the molecular displacement was random. Eq. (24) then becomes

$$k_t = kC[1 - \beta\operatorname{erfc}(y)] , \tag{25}$$

where

$$y = (a/\beta)\sqrt{\pi/t} , \tag{26}$$

and a and β are related to the size and frequency of displacements which can be expressed in terms of D', ρ, and k. In this context, Noyes pair model does not differ from the diffusion model in concept and yet Eqs. (25) and (21) still behave differently. We are interested in comparing these two models with our experimental data. In the concentration diffusion or the Noyes random flights descriptions at least two problems come to mind. One is that the diffusion coefficient in the usual description is assumed to be independent of the separation of A* and D which may be incorrect for the cases in which A* and D are within a few molecular diameters of each other. Second, the motions of A and D may be correlated and not describable by a random walk since the motion of one fragment influences the motion of the solvent molecules which can effect a drag on the other fragment. Furthermore, in these processes it may not be accurate to describe the solvent as a continuous and isotropic medium and therefore motions in certain directions and having certain displacement sizes may be favored.

D. Convolution

In most experimental conditions the laser pulses can be considered as δ pulses. However, in the case that the rate of electron-transfer reaction is very rapid, the finite widths of the light pulses have to be taken into account to avoid ambiguity. For this purpose we rewrite Eq. (3) as

$$\underset{(1-n_A-n_c)}{A + D} \xrightarrow{I(t)} \underset{n_A}{A^*} + D \xrightarrow{f(t)} \underset{n_c}{A^-} - D^+ \xrightarrow{P(t)} A^{-*} - D^+ , \tag{27}$$

where $I(t)$ and $P(t)$ are the exciting and probe pulses, respectively, They can be expressed approximately as Gaussian pulses,[17] i.e.,

$$I(t) = \exp(-t^2/t_e^2) , \tag{28a}$$

$$P(t) = \exp(-t^2/t_p^2) , \tag{28b}$$

where t_e and t_p are, respectively, the half values of the pulse widths of the exciting and probe pulses. The rate equations of Eq. (27) can be given by

$$\dot{n}_A = I(t)(1 - 2n_A - n_c) - f(t)n_A , \tag{29a}$$

$$\dot{n}_c = f(t)n_A . \tag{29b}$$

Here we have not included the decays of A* and A^- because the time range involved in these cases is so short that their decays are negligible. Eq. (29a) and (29b) can be solved numerically for any given $f(t)$. The actual $n_c(t)$ as monitored by the probe pulse is given by $n_c'(t)$,

$$n_c'(t) = \int_0^\infty n_c(t')\exp[-(t - t')^2/t_p^2]dt' . \tag{30}$$

The function $n_c'(t)$ is then substituted into Eq. (13) to obtain the desired expression and be compared with the experimental results.

IV. RESULTS AND DISCUSSION

The hexane solutions of anthracene and diethylaniline whose concentration is varied from 0.1M to 6M (pure

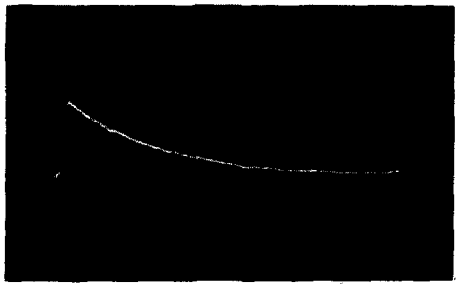

FIG. 5. The fluorescence decay of the charge transfer complex for anthracene ($2.5\times10^{-3}M$) disolved in diethylaniline.

DEA) and the acetonitrile solution of $1M$ and $3M$ DEA have been investigated in this experiment. The absorption spectra of these solutions from 3300 Å to 4000 Å are identical to that of anthracene alone in hexane indicating that there is no significant ground state interaction between anthracene and DEA. In acetonitrile solutions where apparently the ion pair mechanism is operative [Eq. (1)], very little fluorescence from the CT complex can be measured. In contrast strong CT emission is observed in hexane solutions and as DEA concentration is increased the CT emission becomes more intense. At very high DEA concentrations anthracene fluorescence is entirely quenched within our experimental sensitivity. As expected, we also observe the progressing of a solvent-dependent red shift[18] of the CT emission as DEA concentrates in hexane is increased. At higher DEA concentrates, the dielectric constant of the solution is higher and the interaction between solvent and CT complex which is a strong dipolar molecule increases. Consequently, the emitting level is decreased in energy. Whenever the CT emission can be detected by the fast response (0.3 nsec) photodiode, the fluorescence decay is measured directly. A typical decay curve is shown in Fig. 5. For all hexane solutions, the CT complex decay time is about 45 ~ 70 nsec. We should point out that in preparing our samples, we just saturated the solutions with nitrogen without deaerating entirely. The residual oxygen can still quench the CT complex emission. In any event, the lifetime of the complex is so long in comparison with the time range of interest that it does not affect our data analysis.

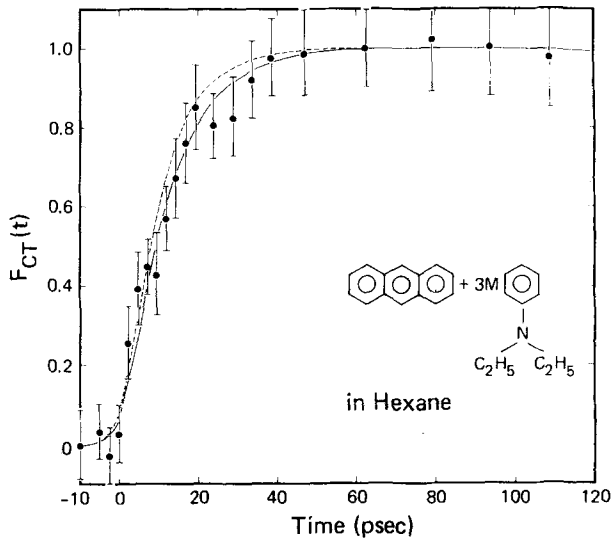

FIG. 7. Analogous result for A and $3M$ DEA in hexane. The rate constants are 9×10^{10} sec^{-1} for solid curve and 11×10^{10} sec^{-1} for dashed curve.

Some of the experimental results, expressed in $F_{CT}(t)$, are shown in Figs. (6)–(12). $F_{CT}(t)$, derived from Eq. (13), is given by

$$F_{CT}(t)=n_c(t)/n_A(0)=[1/\epsilon_c l n_A(0)]\ln(I_0/I_{\parallel})(I_0/I_{\perp})^2 \qquad (31)$$

Except for the hexane solution of A–$(CH_2)_3$–DMA, which will be discussed later, Eq. (8) is directly applicable. The quantity of interest is the rate function $f(t)$. For

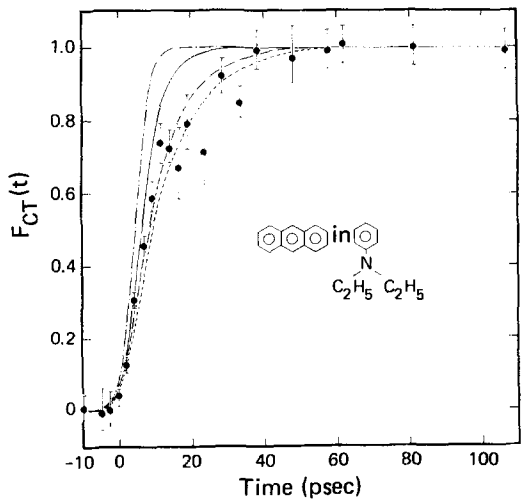

FIG. 6. Charge-transfer complex formation, F_{CT} vs time for A in DEA. The curves are calculated formation function convoluted with the pulse widths of the laser pulses. The rate constant is 9×10^{10} sec^{-1} for ----; 11×10^{10} sec^{-1} for — — —; 22×10^{10} sec^{-1} for ———; $\gtrsim 66\cdot10^{10}$ sec^{-1} for —·—.

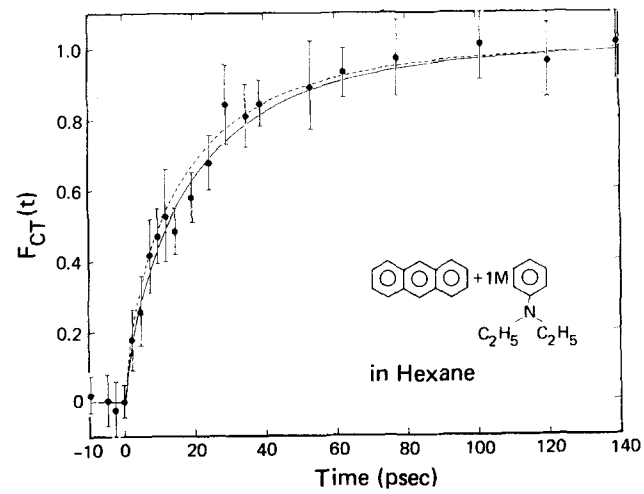

FIG. 8. Analogous result for A and $1M$ DEA in hexane. The solid curve is the formation curve calculated from the diffusion model including all transient terms with $\rho=8$ Å and $k=11\times10^{10}M^{-1}$sec^{-1} and the dashed curve is calculated from the Noyes pair model with same ρ and k.

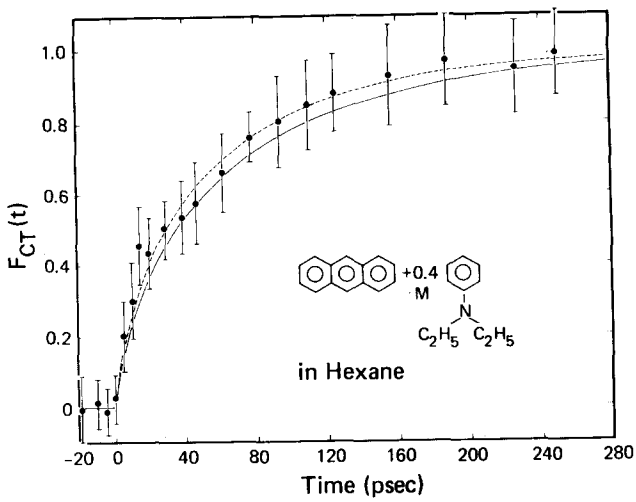

FIG. 9. Analogous result for A and 0.4M DEA in hexane. The solid curve is the formation curve calculated from the diffusion model including all transient terms with $\rho = 8$ Å and $k = 11\times10^{10}M^{-1}$ sec^{-1} and the dashed curve is calculated from the Noyes pair model with same ρ and k.

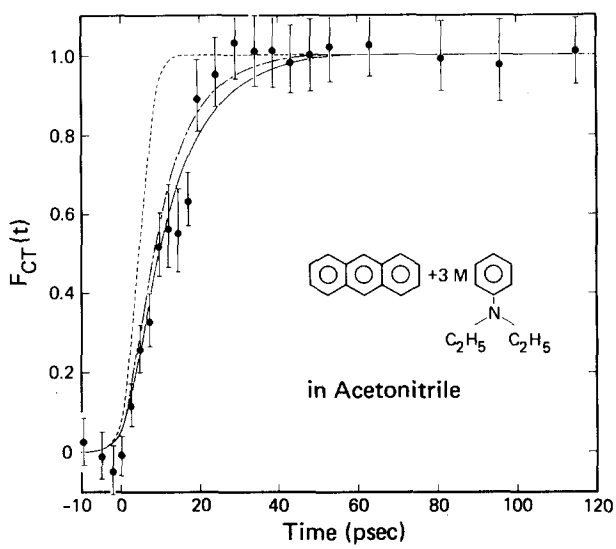

FIG. 11. Ion pair formation for A + 3M DEA in acetonitrile. The curves are calculated formation functions convoluted with the pulse widths of the laser pulses. The rate constant is 9 $\times10^{10}$sec^{-1} for ———; 11×10^{10}sec^{-1} for ——— - ———; $\gtrsim 66\times10^{10}$ sec^{-1} for ----.

clarity, the subsequent discussion is divided into several sections. Interconnections among them will be made freely whenever relevant.

A. Diffusion model, Noyes pair model, and transient behavior

The time dependence for the electron transfer in the diffusion model is obtained by substituting Eq. 21 into Eq. 8. We calculate $D' = D_A + D_{DEA}$ from the known value of $D' = 3.7\times10^{-5}$ cm^2/sec[19] in acetronitrile and the viscosities of the solutions. We adjust two parameters k and ρ to calculate the formation curves and compare them with the experimental data. We find that the rate function from Eq. (21) fits the experimental results very well except those in highest DEA concentrations, i.e., 3M and 6M DEA. In all experiments in which the DEA concentration was less than or equal to 1M the same values for k and ρ were obtained, namely $k = (11\pm1)\times10^{10}M^{-1}$sec^{-1} and $\rho = (8\pm0.5)$ Å. These same values were obtained regardless of whether the solvent was hexane or acetonitrile (Figs. 8, 9, 10, and 12). The significance of the data in highest DEA concentration will be discussed later. The importance of the transient behavior due to the instantaneous flux at the early time becomes immediately evident. To estimate its effect on the rate of reaction, let us take the typical values of k, ρ, and D' from our results and evaluate the second term in Eq. (21). For the value of this term to be 0.1, i.e., 10% of Φ, or less, the time scale has to be 3.7 nsec or longer. For $t = 1$ nsec, corresponding to approximately the time scale of reaction in 0.05M DEA, the effect of the transient terms is about 19%. We see that for DEA concentrations higher than this value, neglect of this term can lead to serious error. Furthermore, for the systems in these studies the inclusion of just the first term in the expansion of $\exp(x^2)\mathrm{erfc}(x)$, as done by Noyes[14] and Ware *et al.*,[15] is definitely inadequate. Again, it can be readily shown that the effect of the second term in the expansion can be reduced to 10% only after 30 psec and 1% after 300 psec. All these effects clearly demonstrate the highly time dependent nature of the reaction process and the importance of the early time behavior. We should point out that physically, this is the consequence of the large reacting radius ρ and the high electron-transfer rate constant k at this distance. If the reacting radius and/or the elementary rate constant is smaller, the effects of transient behavior would be reduced accordingly. As judged from Eq. (21), the concentration of DEA does not seem to affect the relative importance of the transient terms. This actually could be quite misleading. As the concentration of DEA is increased the time range of interaction becomes shorter and consequently the transient effect becomes more important, consistent with our experimental findings.

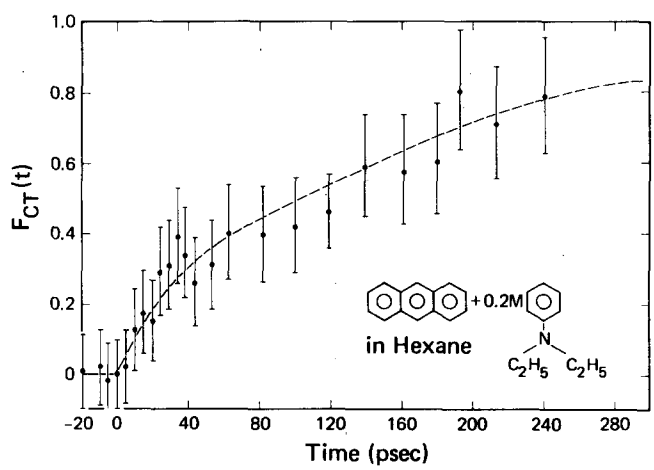

FIG. 10. Analogous result for A + 0.2M DEA in hexane. The dashed curve is calculated from the diffusion model including transient terms with $\rho = 8$ Å and $k = 11\cdot10^{10}M^{-1}$sec^{-1}.

To compare the diffusion and the reacting pair models,

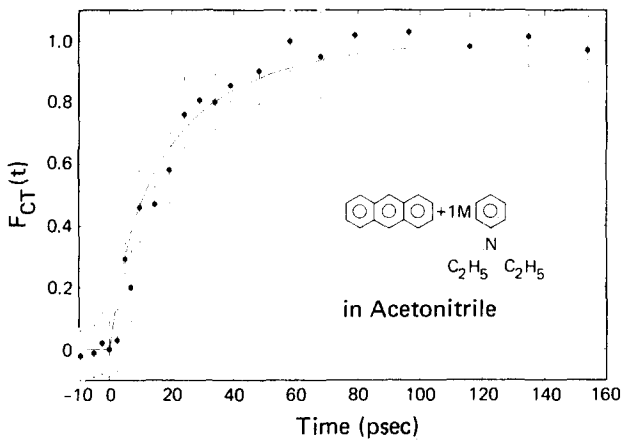

FIG. 12. Analogous result for A + 1M DEA in acetonitrile. The curve is calculated from the diffusion model including all transient terms with $\rho = 8$ Å and $k = 13 \times 10^{10} M^{-1}\text{sec}^{-1}$.

we use the expressions developed by Noyes assuming random flight motion. The parameters a and β in Eq. (26) can then be expressed in terms of D', ρ, and k. The calculated reaction curves from Eqs. (25) and (21) are also shown in Figs. (8) and (9). The two curves converge, as expected, at $t = 0$ and very long time regions. However, at early time regions, i.e., $t \lesssim 10$ psec, the two models can deviate from each other by as much as 10~15% and for a given set of D', ρ, and k, the Noyes pair model always has faster rate of reaction. The discrepancy arises from the fact that only approximate expression is given to the function $h(t)$ and that Noyes equations for a and β in terms of D', ρ, and k are correct only for long time regions where the adoption of the first terms in the expansion of transient terms in Eq. (21) and (25) is valid. For detailed comparison, one would have to obtain expressions for a and β valid for all time ranges. The effort is not warranted, however, if random flight assumption is still to be used for evaluating the probability of encounter, $h(t)$. Indeed, with the known expressions for the two models, we find basically the same values of ρ and k from our experimental data. Unless the function $h(t)$ can be expressed to reflect the nonrandom nature of the system, e.g., solvent–solute interaction, position and direction dependent displacement, preferred orientation of the molecule, etc., the comparison of these two models would not be really fruitful. It is mainly for studying this nonrandom nature of the interactions in liquids, that Noyes developed this reacting pair model and yet because of the complexity of the problem, accurate expression for $h(t)$ still remains to be worked out. In this effort, we have also investigated the cage effect in photodissociation and recombination[20] in order to have a better understanding of fundamental interactions and dynamic processes in liquids.

B. Reorientation motion

To obtain the rate of rotational relaxation in these interacting systems, we use $n_c(t)$ obtained from the previous section and the following equation,

$$Y(t) = (\ln R)/n_c(t) \quad . \tag{32}$$

The result for anthracene and pure DEA is shown in Fig. (13). We find that $Y(t)$ is positive for all t. This indicates that the transition moment of $A^- \rightarrow A^{-*}$ transition in the excited state complex at 6943 Å is perpendicular to the transition moment of $A \rightarrow A^*$ transition at 3472 Å. Since the transition moment of the excited singlet of anthracene ($A_{1g} \rightarrow B_{2u}$) is along the molecular short axis, the $A^- \rightarrow A^{-*}$ transition must be along the molecular long axis. We, therefore, find that the transition moment in the excited state complex at 6943 Å is in agreement with prior measurements of the free anthracene radical anion transition at this energy.[21] We find that $Y(t)$ agrees reasonably well with an exponential function. This strongly indicates from Eq. (19) and (20) that the rotational diffusion constant of the CT complex is not drastically different from that of anthracene. This is not very surprising since the CT complex is basically in a sandwich structure, therefore, the formation of the complex does not alter the diameter of the molecule to a great extent. The orientational relaxation time thus obtained, i.e., $1/6D_c \approx 1/6D_A$ is 60 psec. We compare this value with that calculated from the Debye–Stokes–Einstein hydrodynamic model,[22] i.e.,

$$\tau = \eta V/KT \quad , \tag{33}$$

where η is the viscosity and V is the hydrodynamic volume of the molecule. The orientational relaxation time τ so obtained for anthracene in DEA is about 50 psec and that for the CT complex must be higher. Considering the scattering of experimental data, partly due to the nature of the function $Y(t)$ itself, the agreement between the calculated and experimental values is rather good. We have also compared this value with the rotational relaxation time of A–$(CH_2)_3$–DMA in DEA.[8] The latter has a relaxation time of 80 psec. Since there is no appreciable ground state interaction between A and DEA groups, the molecule is most probably in a stretched conformation. In neat DEA, this molecule forms excited inter- rather than intramolecular CT complex with DEA and thus the methylene and DMA groups apparently have effect on the rotational motion of the molecule.

Besides the anthracene in pure DEA solution, we also observe rotational anisotropy in other solutions. However, as the concentration of DEA is decreased, the observed anisotropy quickly becomes less pronounced, i.e., $\ln R \approx 0$ for all time. This is really understandable because the rate of CT formation becomes slower and the rate of molecular rotation becomes much faster as DEA is diluted by hexane or acetonitrile. For example, for 1M DEA in hexane the viscosity of the solution is only 19.5% of that of pure DEA. The rotational relaxation time would be reduced by more than a factor of 5. Meanwhile, the formation of CT complex is spread over a longer time range. Both factors make the detection of rotational anisotropy more difficult. In view of the importance of geometrical requirements for electron-transfer interactions, the measurement of these orientational relaxation times is really helpful in understanding the dynamic process of the systems.

C. Dynamics of charge-transfer complex and ion pair formation

At a concentration of 1M DEA, the rates of formation of CT complex in hexane and ion pair in acetonitrile are

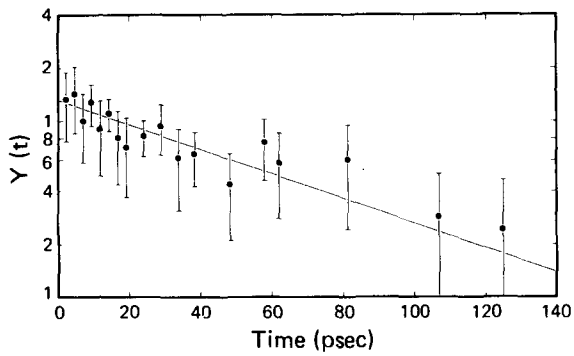

FIG. 13. Plot of Log $Y(t)$ vs time for Å in DEA.

the same. Both solutions follow the transient behavior of diffusion with similar rate constant and critical intermolecular distance for reaction, (Figs. 8 and 12). In the highest DEA concentration region, we find that the reaction rates no longer scale with equilibrium DEA concentration, as suggested by the translational diffusion model, Eq. (21). As shown in Figs. 6, 7, and 11, the growth curves of either the ion pair or the CT complex are very similar for pure DEA and 3*M* DEA in acenitrile and in hexane. Upon convolution with exciting and probe light pulse widths, i.e., Eq. (30), all shows an exponential formation curve with a rate constant $k_{CT} = (10 \pm 1) \times 10^{10}$ sec^{-1}. The same values obtained for the reaction rate constant k_{CT} at 3*M* DEA and in the neat DEA (6*M*) suggests several possibilities. One is a preferential or nonrandom alignment of the DEA molecules about A* in the 3*M* solution, thus leading to the same environment of DEA molecules suitable for electron transfer in both the 3*M* and 6*M* cases. Second, that the lower viscosity in the 3*M* solution leads to a more rapid orientation of A* and DEA into an alignment favorable for electron transfer which roughly compensates for the decreased probability of finding a DEA in the proper configuration in the lower concentration case (3*M*) relative to the neat liquid. The third possibility is that the variations in the pulse widths and the scatter in the data do not permit the reliable determination necessary to separate the early portion of the rise times for the 3*M* and 6*M* cases.

To determine the possible role of orientational effects on electron transfer, we have also studied the rate of CT complex formation of the model molecule A–$(CH_2)_3$–DMA.[8] Here, the A and DMA groups are separated by less than 4 Å due to the methylene bonds, well within the 8 Å found for very rapid (10^{-11} sec) electron transfer. Yet in hexane solutions, intramolecular electron-transfer takes almost a nsec to occur. In this example, we have clearly demonstrated the importance of molecular orientation of the acceptor and donor for interaction in low dielectric solvents. In a separate experiment, we freeze both A and A–$(CH_2)_3$–DMA in pure DEA at liquid nitrogen temperature. In neither case, could we observe the CT complex emission; only the fluorescence due to the excited anthracene was observed. These experimental results suggest a clear picture of reaction dynamics. In these solutions the acceptor (A) is surrounded by many donors (D). Upon excitation, A and the surrounding D molecules have to reorient slightly for electron transfer to occur. Judging from the reorientational relaxation time of the molecule discussed in a previous section, we know that extensive molecular reorientation is not necessary otherwise the process of reaction would be much slower. This conclusion is supported by additional data we have for the A–$(CH_2)_3$–DMA in DEA systems. The reaction rate of this latter system is about 35% slower than that of A and pure DEA system. Meanwhile, rotational relaxation time of A–$(CH_2)_3$–DMA is about 33% longer than that of free A. Of course, in the reaction process both the acceptor and the donor molecules are rotating, not just A. It is therefore clear that the rate of molecular rotation affects the rate of electron-transfer.

V. CONCLUSION

We have employed the technique of picosecond laser photolysis to study the inter- and intramolecular charge-transfer interaction in excited anthracene and *N*,*N*′-diethylaniline systems. We have used a formulation of reaction kinetics coupled with molecular reorientation, so as to analyze the role of both the translational and rotational motions in electron transfer processes. Experimental results show that in lower concentration regions of diethylaniline, reaction kinetics follow the diffusion process with a transient behavior which is induced by the instantaneous flux of particles in early time regions. The values of critical intermolecular distance and primary rate constant for electron transfer are consistent for all solutions studied. Comparison between Noyes reacting pair model and diffusion model is made and discussed. Analysis of orientational relaxation times and the rate of ion pair or charge-transfer complex formation in the high DEA concentration region clearly reveals the dynamic nature of the interacting process. It is shown that relative molecular reorientation is an important and necessary process for electron-transfer in the formation of the excited state charge-transfer complex.

We wish to thank Mr. R. M. Bolding for his assistance in these experiments.

[1] H. Leonhardt and A. Weller, Ber. Bunsenges. Phys. Chem. 67, 791 (1963); A. Weller, Pure Appl. Chem. 16, 115 (1968), and references therein.
[2] E. A. Chandross, J. Ferguson, and E. G. McRae, J. Chem. Phys. 45, 3546 (1966), and references therein.
[3] T. J. Chuang and K. B. Eisenthal, J. Chem. Phys. 59, 2140 (1973).
[4] E. A. Chandross and H. T. Thomas, Chem. Phys. Lett. 6, 393 (1971).
[5] R. Ide, Y. Sakata, S. Misumi, T. Okada, and N. Mataga, Chem. Phys. Lett. 14, 563 (1972).
[6] K. H. Grellmann, A. R. Watkins, and A. Weller, J. Luminescence 1–2, 678 (1970); D. Rehm and A. Weller, Israel J. Chem. 8, 259 (1970).
[7] C. R. Goldschmidt, R. Potashnik, and M. Ottolenghi, J. Phys. Chem. 75, 1025 (1971); N. Orbach, R. Potashnik, and M. Ottolenghi, *ibid.* 76, 1133 (1972).
[8] T. J. Chuang, R. J. Cox, and K. B. Eisenthal, J. Am. Chem. Soc. 96, 6828 (1974).

[9]See, e.g., D. Van der Linde, O. Bernecker, and W. Kaiser, Opt. Comm. 2, 149 (1970).
[10]J. A. Giordmaine, P. M. Rentzepis, S. L. Shapiro, and K. W. Wocht, Appl. Phys. Lett. 11, 216 (1967); P. M. Rentzepis and M. A. Dugnay, *ibid.* 11, 218 (1967).
[11]R. Potashnik, C. R. Goldschmidt, M. Ottolenghi, and A. Weller, J. Chem. Phys. 55, 5344 (1971).
[12]T. J. Chuang and K. B. Eisenthal, J. Chem. Phys. 57, 5094 (1972).
[13]We use the Euler angles defined by H. Goldstein, *Classical Mechanics* (Addison-Wesley, Cambridge, Mass., 1950), p. 107. His (x,y,z) and (x',y',z') are our (Y,X,Z) and (y,x,z), respectively.
[14]R. M. Noyes, Progr. React. Kinet. 1, 129 (1961), and references therein.
[15]W. R. Ware and J. S. Novros, J. Phys. Chem. 70, 3246 (1965).
[16]H. L. Frisch and F. C. Collins, J. Chem. Phys. 20, 1797 (1952).
[17]D. Van der Linde, IEEE J. Quantum Electron. QE-8, 328 (1972).
[18]Von E. Lippert, Z. Elektrochem. 61, 962 (1957).
[19]H. Knibbe, D. Rehm, and A. Weller, Ber. Bunsenges. Phys. Chem. 72, 257 (1968).
[20]T. J. Chuang, G. W. Hoffman, and K. B. Eisenthal, Chem. Phys. Lett. 25, 201 (1974).
[21]G. J. Hoytink and P. J. Zandstra, Mol. Phys. 3, 371 (1960).
[22]P. Debye, *Polar Molecules* (Dover, London, 1924), p. 84.